Available online at www.sciencedirect.com
SCIENCE DIRECT
Bioorganic & Medicinal Chemistry 14 (2006) 5316–5324
Bioorganic & Medicinal Chemistry

Crystallographic studies on *N*-azidoacetyl-β-D-glucopyranosylamine, an inhibitor of glycogen phosphorylase: Comparison with *N*-acetyl-β-D-glucopyranosylamine

Evangelia I. Petsalakis,[a,†] Evangelia D. Chrysina,[a] Costas Tiraidis,[a] Theodoros Hadjiloi,[a] Demetres D. Leonidas,[a] Nikos G. Oikonomakos,[a,b,*] Udayanath Aich,[c] Babu Varghese[d] and Duraikkannu Loganathan[c,*]

[a]*Institute of Organic and Pharmaceutical Chemistry, The National Hellenic Research Foundation, 48, Vas. Constantinou Ave., 116 35 Athens, Greece*
[b]*Institute of Biological Research and Biotechnology, The National Hellenic Research Foundation, 48, Vas. Constantinou Ave., 116 35 Athens, Greece*
[c]*Department of Chemistry, Indian Institute of Technology Madras, Chennai 600 036, India*
[d]*Sophisticated Analytical Instrumentation Facility, Indian Institute of Technology Madras, Chennai 600 036, India*

Received 21 December 2005; revised 20 March 2006; accepted 24 March 2006
Available online 17 April 2006

Abstract—*N*-Acetyl-β-D-glucopyranosylamine (NAG) is a potent inhibitor (K_i = 32 μM) of glycogen phosphorylase b (GPb), and has been employed as a lead compound for the structure-based design of new analogues, in an effort to utilize its potential as a hypoglycaemic agent. Replacement of the acetamido group by azidoacetamido group resulted in an inhibitor, *N*-azidoacetyl-β-D-glucopyranosylamine (azido-NAG), with a K_i value of 48.7 μM, in the direction of glycogen synthesis. In order to elucidate the mechanism of inhibition, we determined the ligand structure in complex with GPb at 2.03 Å resolution, and the structure of the fully acetylated derivative in the free form. The molecular packing of the latter is stabilized by a number of bifurcated hydrogen bonds of which the one involving a bifurcated C–H···N···H–C type hydrogen bonding is rather unique in organic azides. Azido-NAG can be accommodated in the catalytic site of T-state GPb at approximately the same position as that of NAG and stabilizes the T-state conformation of the 280s loop by making several favourable contacts to residues of this loop. The difference observed in the K_i values of the two analogues can be interpreted in terms of desolvation effects, subtle structural changes of protein residues and changes in water structure.

1. Introduction

Design of inhibitors of glycogen phosphorylase (GP) with pharmaceutical applications in improving glycaemic control in type 2 diabetes is a promising therapeutic strategy.[1–8] One of the early successes was the design and synthesis of *N*-acetyl-β-D-glucopyranosylamine (NAG, **1**, Scheme 1), which inhibited GPb activity with a K_i = 32 μM.[9] Extensive physiological studies showed that NAG was an effective inhibitor of liver GPa in rat hepatocytes and that it was able to enhance the dephosphorylation (inactivation) of GPa,[10–12] indicating a potential hypoglycaemic action. Information available from the crystal structures of T-state GPb–NAG complex at 2.3 Å[9,13] and recently at 1.9 Å resolution[14] has shown that NAG fits neatly into the so-called β-pocket, a side channel from the catalytic site, lined by both polar and nonpolar groups,[15] and binding is stabilized through a strong hydrogen bond formed between the amide nitrogen and the main chain carbonyl O of His377. Upon binding at the catalytic site, NAG promotes the (less active) T-state conformation of the enzyme through stabilization of the closed position of 280s loop (residues 282–287), which blocks access of the substrate to the catalytic site. Following crystallographic analysis of NAG complex, a large

Keywords: Type 2 diabetes; Glycogen phosphorylase; *N*-Azidoacetyl-β-D-glucopyranosylamine; Inhibition; X-ray crystallography.
* Corresponding authors. Tel.: +30 210 7273 884x761; fax: +30 210 7273 831 (G.O.); tel.: +91 44 2257 4206; fax: +91 44 2257 0509 (D.L.); e-mail addresses: ngo@eie.gr; loganath@iitm.ac.in
† Present address: Meyerhofstrasse 1, EMBL, D-69117 Heidelberg, Germany.

0968-0896/$ - see front matter © 2006 Elsevier Ltd. All rights reserved.
doi:10.1016/j.bmc.2006.03.044

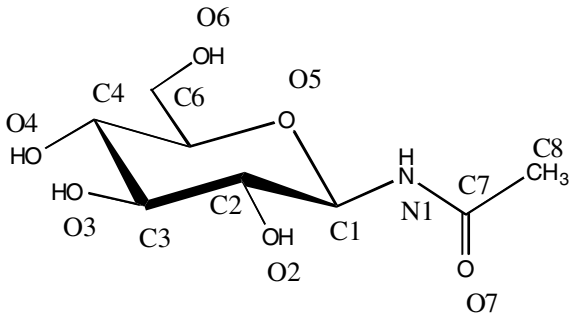

***N*-Acetyl-β-D-glucopyranosyl amine (NAG, 1)**

K_i = 32 ± 1 μM

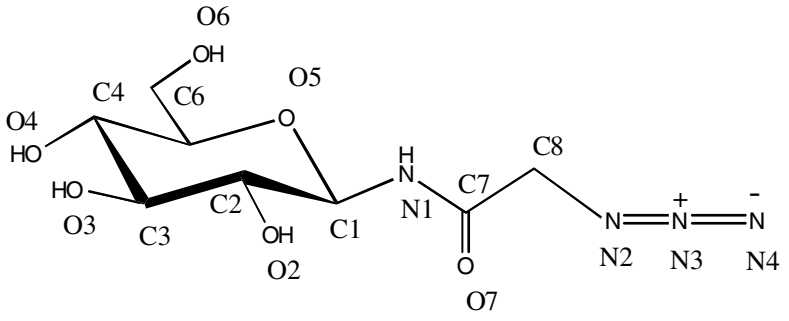

***N*-Azidoacetyl-β-D-glucopyranosyl amine (Azido-NAG, 2)**

K_i = 48.7 ± 4 μM

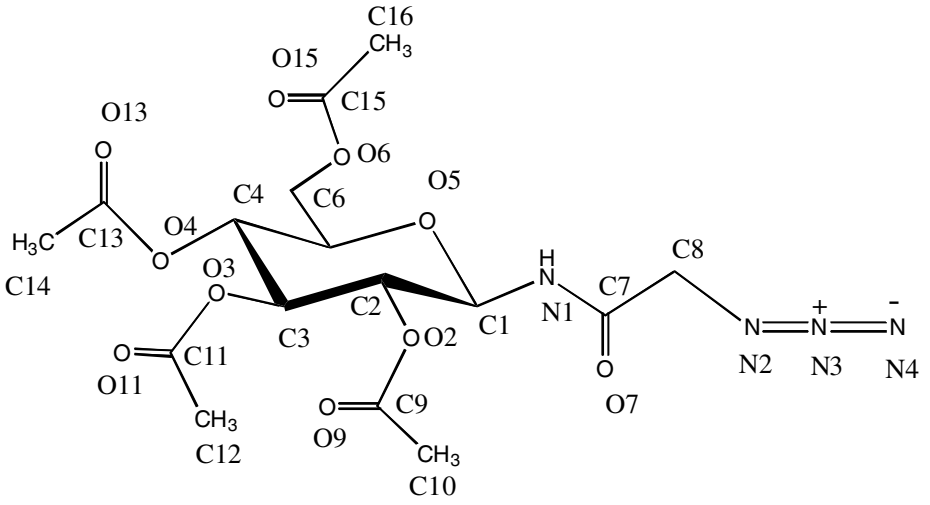

2,3,4,6-Tetra-*O*-acetyl-*N*-azidoacetyl-β-D-glucopyranosyl amine (3)

Scheme 1. Chemical structures of NAG (**1**), azido-NAG (**2**) and the fully acetylated azido-NAG (**3**) showing the numbering system used.

number of derivatives were synthesized and studied by X-ray crystallography with the objective to identify more potent inhibitors, but none of the analogues studied resulted in improved K_i values compared with the lead molecule.[13] Introduction of a large hydrophobic group in the amide nitrogen of NAG led to a more effective inhibitor, *N*-(β-D-glycopyranosyl) 3-(2-naphthyl)propenoic acid amide (K_i = 3.5 μM), but no crystallographic studies have yet been reported.[16] A better understanding of the mechanism of inhibition of GP through identification of the target constraints that are related to the binding affinity of a candidate compound to the β-pocket should aid the design of improved inhibitors against GP.

We report here on the kinetic and crystallographic experiments of *N*-azidoacetyl-β-D-glucopyranosylamine (azido-NAG, **2**, Scheme 1) with GPb. Replacement of the acetyl group, in NAG, by an azidoacetyl group, resulted in a decrease of the inhibitory effect (K_i = 48.7 μM) on

GPb. To substantiate the mechanism of azido-NAG inhibition of the enzyme, we determined the crystal structures of azido-NAG in complex with GPb at 2.03 Å resolution and its acetylated derivative in the free form using X-ray crystallography. The crystallographic results show that azido-NAG, as compared to NAG, on binding to the enzyme, makes additional contacts with the protein at the catalytic site that can provide a rationale for the kinetic properties of the inhibitor.

2. Results and discussion

We have shown previously that NAG (**1**) is an effective competitive inhibitor of GPb with K_i value of 32 (±1) μM.[9] The inhibitory efficiency of azido-NAG (**2**) was tested with GPb. The compound displayed competitive inhibition with respect to the substrate Glc-1-P, at constant concentrations of glycogen (1% w/v) and AMP (1 mM). The inhibition constant of azido-NAG (**2**) for rabbit muscle GPb is $K_i = 48.7 \pm 4.0$ μM, approximately 1.5 times increased than that of NAG, indicating a difference in the binding energy between azido-NAG and NAG of about 0.25 kcal/mol. In order to elucidate the structural basis of this difference in affinity, we have undertaken the crystallographic investigation of GPb in complex with azido-NAG.

A comparative study of the molecular conformation of azido-NAG (**2**) in the free state versus in complex with GPb was initially explored. While the efforts to crystallize azido-NAG using various solvents proved in vain, the corresponding tetra-*O*-acetyl derivative (**3**) crystallized from a mixture of ethyl acetate and hexane as needles suitable for single crystal analysis. The details of crystal data, intensity data collection and structure refinement are given in Table 1. ORTEP depiction with atom numbering is shown in Figure 1 and the selected geometrical parameters are listed in Table 2. The C1–N1 bond length is comparable with a value of 1.431(4) Å reported for NAG.[17] The N2–N3 bond length of the azido group is found to be longer than that of N3–N4. Such a trend has been observed earlier for the corresponding N–N bond lengths (1.234 and 1.130 Å, respectively) in the crystal structure of azidoacetamide.[18]

The orientation of the acetoxy group at C6 is *gg* as evident from the torsion angles of O5–C5–C6–O6 (−67.3°) and C4–C5–C6–O6 (54°). The torsion angles, O5–C1–N1–C7 and C1–N1–C7–C8, are −111.9° and −171.5°, respectively, which point out the *Z-anti*-conformation of the acetamido moiety. The conformation about the C7–C8 bond is *syn* with respect to the amido nitrogen (N1) and the azide group as shown by the torsion angle N1–C7–C8–N2 (6.5°). The value of the corresponding torsion angle in the case of simple azidoacetamide[18] has been reported to be −2.9°.

Careful analysis of the crystal packing was carried out in an effort to identify the key features governing the molecular assembly of the fully acetylated azido-NAG (**3**). Parameters of the various hydrogen bonds observed are listed in Table 3. Barring a single regular hydrogen bond involving N1–H and O7, all other intermolecular interactions are mediated by C–H···O/N hydrogen bonds. Each of the two electron-rich nitrogens, N2 and N4 of the azide groups is involved in a bifurcated acceptor-type interaction with C1–H1 and C3–H3 and C12–H12A and C14–H14B, respectively (Fig. 2). To the best of our knowledge, such bifurcated C–H···N···H–C type hydrogen bonding in organic azides has not been reported. The carbonyl oxygen, O7, is also involved in bifurcated acceptor type hydrogen bonding with N1–H1N and C12–H12C. Furthermore, the direct and bifurcated types of C–H interactions involving O6, O11 and O15 as acceptors lend further stability to the molecular packing.

Table 1. Data collection and refinement parameters for the fully acetylated azido-NAG (**3**)

Parameter	Compound **3**
Empirical formula	$C_{16}H_{22}N_4O_{10}$
Formula weight	430.38
Temperature	293(2) K
Wavelength	0.71073 Å
Crystal system space group	$P2_12_12_1$, orthorhombic
Unit cell dimensions	$a = 8.610(5)$ Å, $b = 12.656(2)$ Å, $c = 19.054(4)$ Å
Volume	2076.1(12) A^3
Z	4
Calculated density	1.377 mg/m^3
Absorption coefficient	0.116 mm^{-1}
$F(000)$	904
Crystal size	$0.3 \times 0.2 \times 0.2$ mm
Theta range for data collection	2–25°
Index ranges	$0 \leqslant h \leqslant 10$, $0 \leqslant k \leqslant 15$, $0 \leqslant l \leqslant 22$
Reflections collected/unique	2085/2085 [R(int) = 0.0000]
Completeness to 2 theta	99.8%
Refinement method	Full-matrix least-squares on F^2
Data restraint parameters	2085/0/275
Goodness-of-fit on F^2	1.022
Final R indices [2⟨sigma⟩ (I)]	$R_1 = 0.0373$, $wR_2 = 0.0981$
R indices (all data)	$R_1 = 0.0729$, $wR_2 = 0.1206$

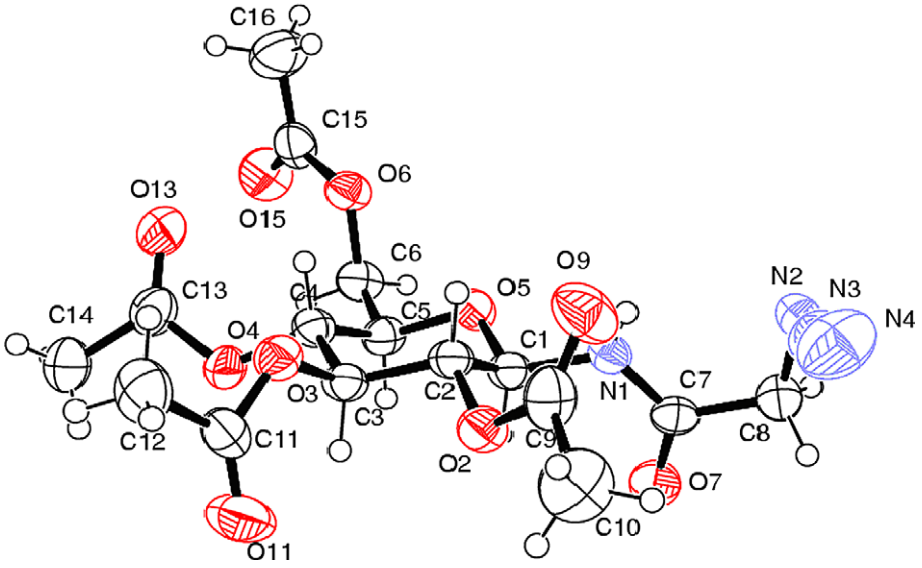

Figure 1. ORTEP (50% probability level) with atom numbering of the fully acetylated azido-NAG (**3**).

Table 2. Selected geometrical parameters for the fully acetylated azido-NAG (**3**)

Bond length	
C1–N1	1.431(5)
C8–N2	1.466(6)
C1–O5	1.425(5)
C5–O5	1.440(5)
N2–N3	1.224(6)
N3–N4	1.137(6)
Bond angle	
N2–N3–N4	172.6(5)
Torsion angle	
O5–C1–N1–C7	−111.9(4)
O5–C5–C6–O6	−67.3(4)
C4–C5–C6–O6	54.0(5)
C1–N1–C7–C8	−171.5(4)
N1–C7–C8–N2	6.5(5)

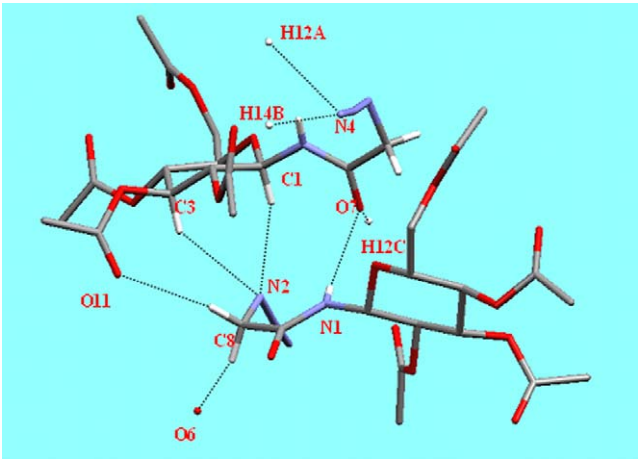

Figure 2. The molecular packing of the fully acetylated azido-NAG (**3**) displaying several C–H···N and C–H···O interactions. Many of the hydrogen atoms are omitted for clarity.

The crystal structure of GPb in complex with azido-NAG was then determined. A summary of the crystallographic data processing and refinement statistics is given in Table 4. A schematic representation of the native T-state structure of GPb indicating the location of the catalytic binding site is shown in Figure 3. Electron density maps defined the position of the inhibitor within the catalytic site (Fig. 4), consistent with the kinetic results. In the bound structure, the torsion angle C7–C8–N2–N3 is 121° (Fig. 5). In contrast, the conformation of the azido moiety about the C8–N2 is observed to be 98° in the single crystal structure of the fully acetylated derivative. Incidentally, the primary hydroxyl group adopts nearly the same conformation, gauche (*gg*), in both structures

Table 3. The molecular packing of the fully acetylated azido-NAG (**3**)

Hydrogen bonds	*d*(D–H)	*d*(H–A)	*d*(D–A)	⟨DHA	Symmetry code
N1–H1N···O7	0.76(0)	2.43(1)	3.081(1)	145.2(2)	$x + 1/2, -y + 1/2, -z + 1$
C12–H12C···O7	0.96(0)	2.70(0)	3.585(1)	152.5(1)	$-x - 1/2, -y, +z - 1/2$
C8–H8A···O6	0.97(0)	2.54(0)	3.366(1)	142.8(2)	$x - 1/2, -y + 1/2, -z + 1$
C8–H8B···O11	0.97 (0)	2.62(0)	3.504(1)	151.6(1)	$x + 1/2, -y + 1/2, -z + 1$
C1–H1···N2	0.98(0)	2.49(1)	3.405(2)	154.6(2)	$x - 1/2, -y + 1/2, -z + 1$
C3–H3···N2	0.98(0)	2.72(1)	3.548(1)	142.4(1)	$x - 1/2, -y + 1/2, -z + 1$
C12–H12A···N4	0.96(0)	2.64(1)	3.482(1)	146.3(2)	$-x, +y - 1/2, -z + 1/2$
C14–H14B···N4	0.96(0)	2.71(0)	3.466(0)	135.9(1)	$x, +y - 1, +z$
C5–H5···O15	0.98(0)	2.52(0)	3.229(1)	129.6(1)	$x - 1/2, -y - 1/2, -z + 1$
C12–H12B···O15	0.96(0)	2.54(0)	3.349(0)	142.5(1)	$-x, +y + 1/2, -z + 1/2$

Table 4. Diffraction data and refinement statistics for GPb–azido-NAG complex

Experiment	100 mM azido-NAG/4h soak
Space group	$P4_32_12$
No. of images (°)	111 (0.8)[a]
Unit cell dimensions (Å)	$a = b = 128.6$, $c = 116.2$
Resolution range (Å)	29.48–2.03
No. of observations	861,420
No. of unique reflections	62,829
$\langle I/\sigma(I)\rangle$ (outermost shell)[b]	19.8 (4.9)
Completeness (outermost shell) (%)	99.1 (98.6)
R_m (outermost shell)[c]	0.069 (0.563)
Outermost shell (Å)	2.06–2.03
Redundancy (outermost shell)	7.4 (7.5)
Refinement (resolution) (Å)	29.48–2.03
No. of reflections used (free)	62,790 (3172)
Residues included	(12–254), (261–314), (324–836)
No. of protein atoms	6590
No. of water molecules	358
No. of ligand atoms	15 (PLP), 18 (azido-NAG)
Final $R(R_{free})$[d] (%)	18.4 (19.9)
R (R_{free}) (outermost shell) (%)	23.8 (25.3)
Outermost shell in refinement (Å)	2.10–2.03
rmsd in bond lengths (Å)	0.006
rmsd in bond angles (°)	1.2
rmsd in dihedrals (°)	21.7
rmsd in impropers (°)	0.85
Average B(Å^2) for residues	(12–254), (261–314), (324–836)
Overall	31.4
CA,C,N,O	29.4
Side chain	33.3
Average B (Å^2) for ligands	19.8 (PLP), 26.6 (azido-NAG)
Average B (Å^2) for water molecules	40.8

[a] 0.8 is the rotation range per image.
[b] $\sigma(I)$ is the standard deviation of I.
[c] $R_{merge} = \sum_i \sum_h |\langle I_h\rangle - I_{ih}|/\sum_i \sum_h I_{ih}$, where $\langle I_h\rangle$ and I_{ih} are the mean and ith measurement of intensity for reflection h, respectively.
[d] Crystallographic $R = \sum||F_o| - |F_c||/\sum|F_o|$, where $|F_o|$ and $|F_c|$ are the observed and calculated structure factor amplitudes, respectively. R_{free} is the corresponding R value for a randomly chosen 5% of the reflections that were not included in the refinement.

(torsion angle O5–C5–C6–O6 is −57° for the GPb–azido-NAG complex and −67° for the free compound **3**). The torsion angle N1–C7–C8–N2 is 179°. Thus, the conformation about the C7–C8 bond with respect to the amido nitrogen (N1) and the azide group turns out to be *anti* for the GPb–azido-NAG complex. The water structure within the catalytic site appears to play a significant role in stabilizing the ligand conformation (see below).

The mode of binding and the interactions that azido-NAG makes with GPb are similar to those described previously for the lead molecule in the 1.9 Å resolution structure of the GPb–NAG complex.[14] The hydrogen bond of the amide nitrogen (N1) with His377 O is retained, an interaction that is conserved in all β-D-glucopyranosylamine[13,14,19,20] and spirohydantoin analogues[21–23] of β-D-glucopyranose studied so far and also the compound 2-(β-D-glucopyranosyl)-benzimidazole.[30] There are five additional hydrogen bonds in comparison to the GPb–NAG complex. N2, N3 and N4 atoms of the azido group [–N=N$^+$=N$^-$] make water-mediated interactions that involve residues Asn282, Asn284 and Phe285 of the 280s loop (residues 282–287), and Ala383 of the 380s loop (residues 377–384) (Table 5). In addition N4 is directly hydrogen bonded to His341 NE2 of the β-pocket, a sub-channel lined by both polar and nonpolar groups, with no access to the bulk solvent.[15] The nitrogen atoms of the azido group are involved in 11 van der Waals interactions with the GPb molecule. These contacts promote the closed geometries and give rise to increased rigidity of the 280s and 380s loops occurring in the T-state GPb. The hydrogen bonds formed between the azido-NAG and the protein are illustrated in Figure 6. There are in total 19 hydrogen bonds and 84 van der Waals interactions (7 nonpolar–nonpolar, 21 polar–polar, and 56 nonpolar/polar) (Table 6) in the GPb–azido-NAG complex. In the GPb–NAG complex there are in total 15 hydrogen bonds and 61 van der Waals interactions (6 nonpolar/nonpolar, 10 polar/polar, and 45 nonpolar/polar).[14] It is likely that some of these contacts particularly those between N4···CE1 His341 (3.1 Å) and C8···OD1 Asn284 (3.3 Å) represent CH···N/O interactions. As shown earlier, the acceptor and donor atoms, N4 and C8, of the fully acetylated azido-NAG (**3**) are also involved in C–H···N/O interactions (Table 3). Although the solid-state conformation of the azidoacetamide moiety in the free and GPb-bound forms of azido-NAG (**2**) may be different, the above results reveal the potential of N4 and C8 to be involved in C–H···N/O interactions.

A structural comparison between the GPb–NAG complex and the GPb–azido-NAG complex shows that the

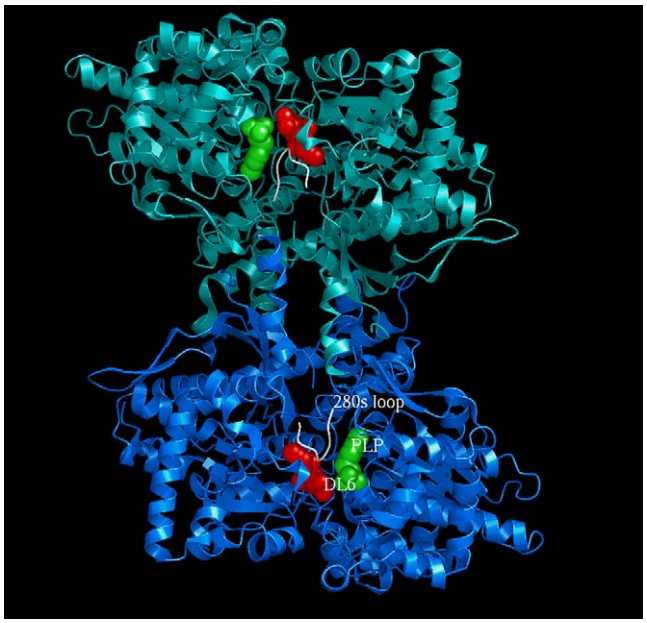

Figure 3. A schematic diagram of the GPb dimeric molecule, viewed down the molecular dyad. One subunit is coloured in blue and the other in cyan. The position is shown for the catalytic site. The catalytic site, marked by azido-NAG (shown in red) and the essential cofactor pyridoxal 5′-phosphate (PLP) (shown in green), is buried at the centre of the subunit and is accessible to the bulk solvent through a 15 Å long channel. Azido-NAG, on binding at the catalytic site promotes the less active T-state through stabilization of the closed position of the 280s loop (shown in white).

two proteins have very similar overall structures (Fig. 7); the positions of the Ca, main-chain and side-chain atoms for well-defined residues (24–249, 261–313 and 326–549, and 558–830) deviate from their mean positions by 0.093, 0.124 and 0.565 Å, respectively, indicating overall negligible changes. At the catalytic site, comparison reveals a conformational shift for residue Asp339; in the GPb–azido-NAG complex (as compared with the GPb-NAG complex), the CG, OD2, and OD1 of Asp339 are shifted ~0.5, 0.9 and 1.3 Å, respectively (the dihedral angle $\chi 2$ [CA–CB–CG–OD1] is rotated by 110°), in order to avoid close contacts with nitrogen N4 atom of azido-NAG. In addition, on ligand binding,

Table 5. Hydrogen bond interactions between azido-NAG and residues at the catalytic site of GPb

Inhibitor atom	GPb–azido-NAG	
	Protein atom	Distance (Å)
N1	His377 O	2.8
O2	Asn284 ND2	3.0
	Tyr573 OH	3.1
	Glu672 OE1	3.2
	Wat99	2.7
	Wat222	3.2
O3	Glu672 OE1	2.6
	Ser674 N	3.2
	Gly675 N	3.0
O4	Gly675 N	2.7
	Wat307	2.7
O6	His377 ND1	2.7
	Asn484 OD1	2.8
O7	Asn284 ND2	3.3
	Wat218	2.5
	Wat310	2.8
N2	Wat310	2.6
N3	Wat275	3.3
	Wat310	3.0
N4	His341 NE2	2.8
	Wat331	2.7

Water mediated interactions. Wat99 is hydrogen-bonded to Thr671 O, Ala673 N, Wat104 and Wat358; Wat358 is in turn hydrogen-bonded to Thr671 O. Wat104 is hydrogen-bonded to Thr671 O, Val379 N, and Wat101. Wat101 is hydrogen-bonded to Gly670 O and to Glu672 O, Asp693 OD2 and Gly694 N through Wat107. Wat222 is hydrogen-bonded to Asn284 ND2, Tyr573 OH, Lys574 NZ, Asp283 OD2, and to Gly135 N, and Asp283 OD1 through Wat59. Wat307 is hydrogen-bonded to Thr676 N and OG1, and PLP O3. Wat218 is hydrogen-bonded to Leu136 N, Asp283 OD, Wat59, and Wat310. Wat310 is hydrogen-bonded to Asn284 N, Wat275 and to Glu88 OE1 and OE2, Asn133 ND2, and Asn282 O through Wat291. Wat275 is hydrogen-bonded to Asn284 N, Phe285 N and O, and Ala383 O through another water molecule (Wat164). Wat331 is hydrogen-bonded to Ala383, and Wat164.

the side chain of Leu136 is rotated by ~107° (dihedral angle $\chi 2$ (CA–CB–CG–CD1)) to optimize contacts with the azido group. Wat331 (Wat110 in the NAG complex

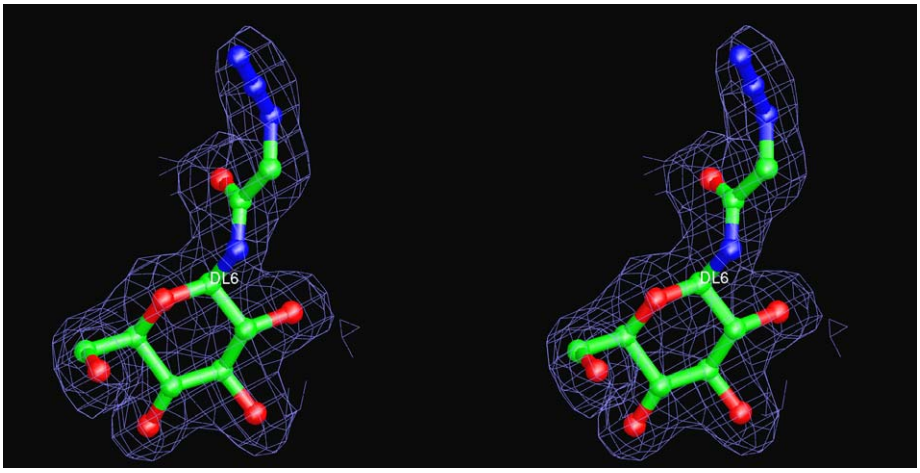

Figure 4. $2F_o - F_c$ electron density map of the refined azido-NAG structure bound at the catalytic site of GPb. The map is contoured at 1.0 σ level.

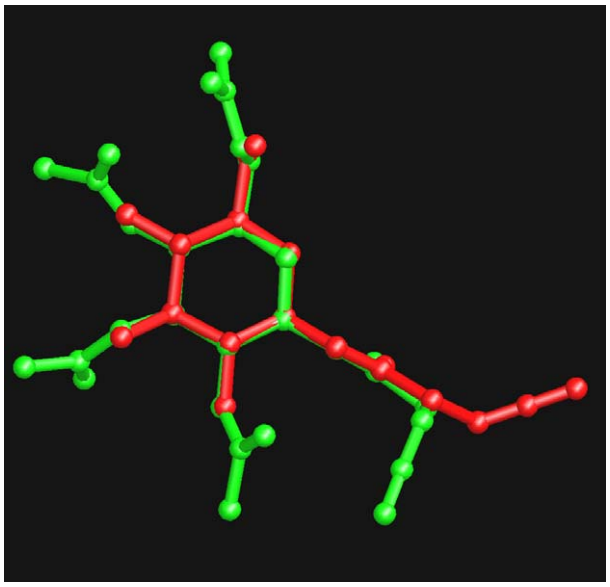

Figure 5. Superposition of the acetylated azido-NAG structure as defined by small molecule X-ray crystallography (shown in green) with the azido-NAG (shown in red) when bound at the catalytic site of GPb.

structure) also shifts by ~1.6 Å to avoid clashes with N4. Furthermore, Wat164 and Wat310 (Wat 109 and Wat355, respectively, in the NAG complex structure) shift away ~0.4 Å from the ligand to create more space for the azido group to be accommodated without causing steric hindrance. Examination of the azido-NAG complex structure reveals a newly recruited water molecule, Wat275, which contacts N3 of the azido group and Asn284 N, Phe285 N and O, and Ala383 O (through Wat164); this water molecule is not detected in the NAG complex structure. The hydrogen bonding interactions of the azido group with existing water molecules and recruitment of a new water molecule that becomes involved in hydrogen bonding networks may provide additional enthalpic interactions (Fig. 6).

The azido-NAG analogue binds with a 1.5-fold decreased affinity relative to the lead compound NAG. The decrease in binding energy associated with azido-substitution of the acetyl group of NAG is however paradoxical with respect to the increased number of hydrogen bonds and van der Waals contacts. It is possible that, in the GPb–azido-NAG complex, the energy gain due to the additional hydrogen bonds and van der Waals interactions is outbalanced by the energy required to desolvate the polar azido group in order to transfer it to the catalytic site. Another explanation for the energy difference (approx 0.25 kcal/mol) may lie in energy loss due to the ligand conformational entropy, as well as to the subtle conformational changes, that cannot be alleviated by a significant improvement on the ligand-catalytic site interactions.

3. Supplementary information

Complete structural data of compound **3** (CCDC # 289270) have been deposited at the Cambridge Crystallographic Data Centre which can be obtained free of charge via www.ccdc.cam.ac.uk/conts/retrieving.html (or from the Cambridge Crystallographic Data Centre, 12 Union Road, Cambridge CB21EZ, UK; fax: (+44) 1123-336-033; or email:deposit@ccdc.cam.ac.uk).

4. Materials and methods

The synthesis of azido-NAG (**2**) (Scheme 1) and *N*-azidoacetyl-2,3,4,6-tetra-*O*-acetyl-β-D-glucopyranosylamine (**3**) was described previously.[24] The latter compound was crystallized from a mixture of ethyl acetate and hexane by the slow evaporation method, whereas efforts to

Table 6. Van der Waals interactions between azido-NAG and residues at the catalytic site of GPb

Inhibitor atom	GPb–azido-NAG	
	Protein atom	No. of contacts
C1	His377 O; Wat218	2
N1	Asn284 OD1, ND2; His377 C, CB	4
C2	His377 O; Glu672 OE1; Wat99; Wat222	4
O2	Asn284 CG, OD1; His377 O	3
C3	Glu672 OE1; Gly675 N; Wat307	3
O3	Glu672 CG,CD; Ala673 N; Ser674 C, CA; Gly675 CA	6
C4	Gly675 N; Wat307	2
O4	Asn484 OD1; Ser674 C, CB; Gly675 C, CA, O; Thr676 N,CG2	8
C5	Gly135 C; Leu136 N; Wat307	3
O5	Leu136 N; His377 CB, CG, O, ND1	5
C6	Gly135 C, O; Leu139 CD2; His377 ND1; Asn484 OD1	5
O6	Leu139 CD2; His377 CG, CE1; Val455 CB,CG1,CG2; Asn484 CG	7
C7	Asn284 CG, OD1, ND2; His377 O,CB; Wat218; Wat310	7
O7	Leu136 CB; Asn284 CG,ND2	3
C8	Asn284 CG, OD1, ND2; His377 O; Thr378 CB; Wat310	6
N2	Asn284 CG,OD1,N,CA; Wat275	5
N3	Leu136 CD1; Asp339 OD2; His341 NE2; Wat331	4
N4	Leu136 CD1; Asp339 CG,OD2; His341 CE1; Wat164; Wat275; Wat310	7
	Total	84

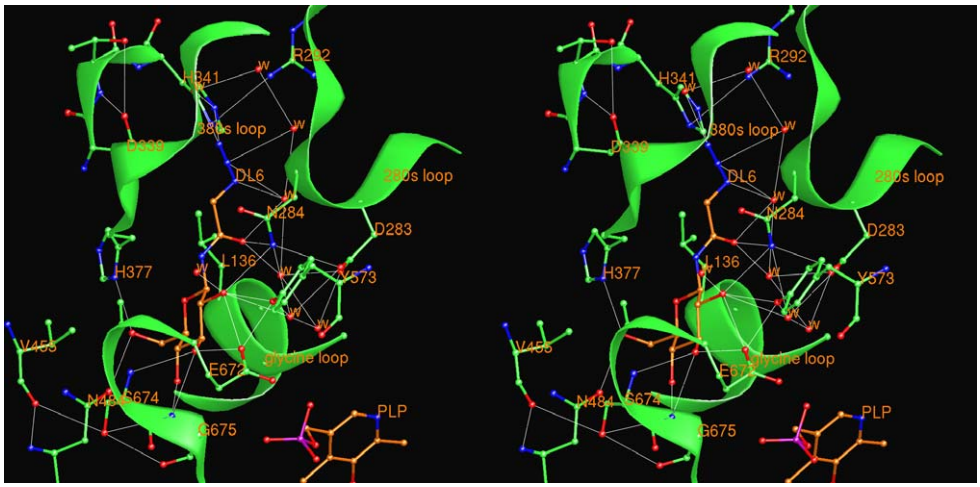

Figure 6. Stereo diagram showing interactions between azido-NAG and protein in the vicinity of the catalytic site. The hydrogen bond pattern between azido-NAG, protein residues, and water molecules (w) in the catalytic site is represented by dotted lines.

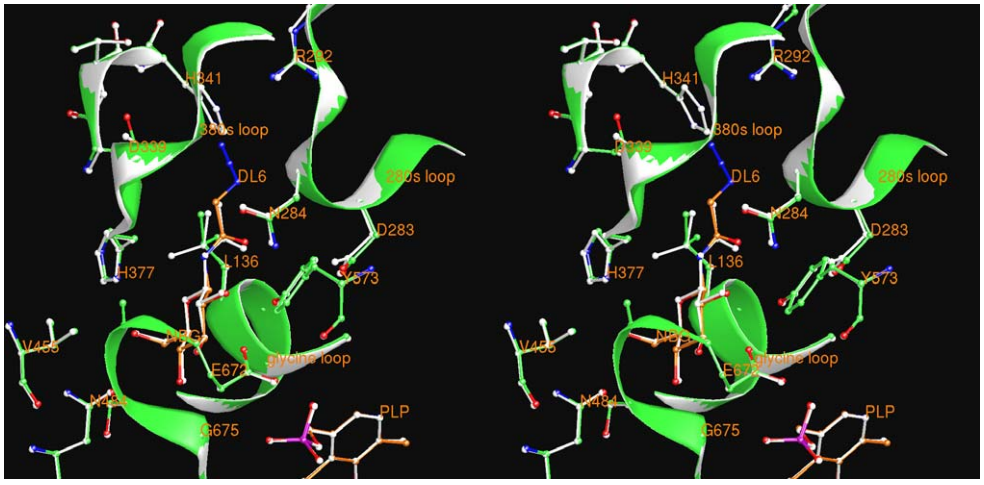

Figure 7. Stereo diagram of the superimposed structures of azido-NAG complex (green) onto NAG (white) in the vicinity of the catalytic site.

obtain the former in crystalline form from several solvent systems proved in vain. X-ray diffraction data were collected at room temperature in the $\omega - 2\theta$ scan mode on an Enraf-Nonius CAD4 diffractometer and the data collection and refinement parameters are given in Table 1. The structure was solved by direct methods using SHELXS-97 and the refinement was done by full matrix using SHELXL-97.[25] ORTEP of the compound was drawn using WinGX[26] and the packing diagrams using Mercury 1.4, provided by CCDC, Cambridge.

Rabbit muscle GPb was isolated, purified, recrystallized and assayed as described.[9] Kinetic experiments were performed in the direction of glycogen synthesis in the presence of constant concentrations of glycogen (1% w/v), AMP (1 mM), and various concentrations of Glc-1-P and inhibitor.[14]

Native T-state GPb crystals, grown in the tetragonal lattice, spacegroup $P4_32_12$,[27] were soaked with 100 mM azido-NAG (for 4 h) in a buffered solution (10 mM Bes, 0.1 mM EDTA and 0.02% sodium azide, pH 6.7), prior to data collection. Data for GPb–azido-NAG complex were collected from a single crystal on Station 9.6 at Daresbury Laboratory to 2.03 Å resolution ($\lambda = 0.87$ Å). The reflections were recorded on an ADSC Q4 CCD detector. Data reduction and integration followed by scaling and merging of the intensities obtained was performed with Denzo and Scalepack, respectively, as implemented in HKL suite.[28]

Crystallographic refinement was performed with CNS version 1.1[29] using positional and individual B-factor refinement with bulk-solvent correction. The crystal structure of GPb in complex with oxadiazole at 1.92 Å resolution[30] was employed as starting model for refinement against the experimental data of GPb–azido-NAG complex. Electron density maps, $(2F_o - F_c)$ and $(F_o - F_c)$, were then calculated and indicated that azido-NAG was tightly bound at the catalytic site of GPb. The azido-NAG model was built using the coordinates from the single crystal structure of the fully acetylated azido-NAG (**3**) and was fitted manually in the electron density. Alternate cycles of manual rebuilding with the program 'O'[31] and refinement with CNS improved the quality of the model. The stereochemistry

of the protein residues was validated by PROCHECK.[32,33] Hydrogen bonds and van der Waals interactions were calculated with the program CONTACT as implemented in CCP4[33] applying a distance cut-off 3.3 and 4.0 Å, respectively. The Luzatti plot[34] suggests an average positional error of approximately 0.22 Å.

Protein structures were superimposed using LSQKAB.[33] The schematic representation of the crystal structures presented in all figures was prepared with the program XOBJECTS (M.E.M. Noble, unpublished results). The coordinates of the new structure have been deposited with the RCSB Protein Data Bank (http://www.rcsb.org/pdb) with the code 2FFR.

Acknowledgments

This work was supported by Greek GSRT through ENTER-EP6/2001, and Scientific and Technological cooperation between Greece and USA (2005-2006), and SRS Daresbury Laboratory (contract IHPP HPRI-CT-1999-00012). We also wish to acknowledge the assistance of Ms. Magda N. Kosmopoulou for help in enzyme crystallization. The authors (D.L. and U.A.) thank the Sophisticated Analytical Instrumentation Facility (SAIF), IIT Madras for the X-ray data collection. One of us (U.A.) is thankful to the Council of Scientific and Industrial Research (CSIR), New Delhi, for award of a Junior Research Fellowship.

References and notes

1. Aiston, S.; Hampson, L.; Gómez-Foix, A. M.; Guinovart, J. J.; Agius, L. *J. Biol. Chem.* **2001**, *276*, 23858–23866.
2. McCormack, J. C.; Westergaard, N.; Kristiansen, M.; Brand, C. L.; Lau, J. *Curr. Pharm. Des.* **2001**, *7*, 1451–1474.
3. Treadway, J. L.; Mendys, P.; Hoover, D. J. *Expert Opin. Investig. Drugs* **2001**, *10*, 439–454.
4. Latsis, T.; Andersen, B.; Agius, L. *Biochem. J.* **2002**, *368*, 309–316.
5. Oikonomakos, N. G. *Curr. Protein Pept. Sci.* **2002**, *3*, 561–586.
6. Aiston, S.; Coghlan, M. P.; Agius, L. *Eur. J. Biochem.* **2003**, *270*, 2773–2781.
7. Somsák, L.; Nagy, V.; Hadady, Z.; Docsa, T.; Gergely, P. *Curr. Pharm. Des.* **2003**, *9*, 1177–1189.
8. Somsák, L.; Nagy, V.; Hadady, Z.; Felföldi, N.; Docsa, T.; Gergely, P. In *Frontiers in Medicinal Chemistry*; Reitz, A. B.; Kordik, C. P.; Choudhary, M. I.; Atta ur Rahman, Eds; Bentham, 2005; Vol. 2, pp 253–272.
9. Oikonomakos, N. G.; Kontou, M.; Zographos, S. E.; Watson, K. A.; Johnson, L. N.; Bichard, C. J. F.; Fleet, G. W. J.; Acharya, K. R. *Protein Sci.* **1995**, *4*, 2469–2477.
10. Board, M.; Hadwen, M.; Johnson, L. N. *Eur. J. Biochem.* **1995**, *228*, 753–761.
11. Board, M.; Bollen, M.; Stalmans, W.; Kim, Y.; Fleet, G. W. J.; Johnson, L. N. *Biochem. J.* **1995**, *311*, 845–852.
12. Board, M.; Johnson, L. N. *Diabetes Res.* **1995**, *28*, 95–109.
13. Watson, K. A.; Mitchell, E. P.; Johnson, L. N.; Cruciani, G.; Son, J. C.; Bichard, C. J. F.; Fleet, G. W. J.; Oikonomakos, N. G.; Kontou, M.; Zographos, S. E. *Acta Crystallogr., D* **1995**, *51*, 458–472.
14. Anagnostou, E.; Kosmopoulou, M. N.; Chrysina, E. D.; Leonidas, D. D.; Hadjiloi, T.; Tiraidis, C.; Györgydeák, Z.; Somsák, L.; Docsa, T.; Gergely, P.; Oikonomakos, N. G. *Bioorg. Med. Chem.* **2006**, *14*, 181–189.
15. Martin, J. L.; Veluraja, K.; Johnson, L. N.; Fleet, G. W. J.; Ramsden, N. G.; Bruce, I.; Oikonomakos, N. G.; Papageorgiou, A. C.; Leonidas, D. D.; Tsitoura, H. S. *Biochemistry* **1991**, *30*, 10101–10116.
16. Györgydeák, Z.; Hadady, Z.; Felföldi, N.; Krakomperger, A.; Nagy, V.; Tóth, M.; Brunyánszki, A.; Docsa, T.; Gergely, P.; Somsák, L. *Bioorg. Med. Chem.* **2004**, *12*, 4861–4870.
17. Sriram, D.; Sreenivasan, H.; Srinivasan, S.; Priya, K.; Vishnu Thirtha, M.; Loganathan, D. *Acta Crystallogr., C* **1997**, *53*, 1075–1077.
18. Kumasaki, M.; Kinbara, K.; Wada, Y.; Arai, M.; Tamura, M. *Acta Crystallogr., E* **2001**, *57*, 6–8.
19. Chrysina, E. D.; Oikonomakos, N. G.; Zographos, S. E.; Kosmopoulou, M. N.; Bischler, N.; Leonidas, D. D.; Kovács, L.; Docsa, T.; Gergely, P.; Somsák, L. *Biocatal. Biotransform.* **2003**, *21*, 233–242.
20. Chrysina, E. D.; Kosmopoulou, M. N.; Kardakaris, R.; Bischler, N.; Leonidas, D. D.; Kannan, T.; Loganathan, D.; Oikonomakos, N. G. *Bioorg. Med. Chem.* **2005**, *13*, 765–772.
21. Bichard, C. J. F.; Mitchell, E. P.; Wormald, M. R.; Watson, K. A.; Johnsosn, L. N.; Zographos, S. E.; Koutra, D. D.; Oikonomakos, N. G.; Fleet, G. W. J. *Tetrahedron Lett.* **1995**, *36*, 2145–2148.
22. Gregoriou, M.; Noble, M. E. M.; Watson, K. A.; Garman, E. F.; Krulle, T. M.; Fuente, C.; Fleet, G. W. J.; Oikonomakos, N. G.; Johnson, L. N. *Protein Sci.* **1998**, *7*, 915–927.
23. Watson, K. A.; Chrysina, E. D.; Tsitsanou, K. E.; Zographos, S. E.; Archontis, G.; Fleet, G. W. J.; Oikonomakos, N. G. *Proteins* **2005**, *61*, 966–983.
24. Aich, U.; Loganathan, D. *J. Carbohydr. Chem.* **2005**, *24*, 1–12.
25. Sheldrick, G. M. *SHELX97: Program for the refinement of crystal structures*; University of Gottingen; Gottingen, Germany, 1997.
26. Farrugia, L. J. *J. Appl. Crystallogr.* **1999**, *32*, 837–838.
27. Oikonomakos, N. G.; Melpidou, A. E.; Johnson, L. N. *Biochim. Biophys. Acta* **1985**, *832*, 248–256.
28. Otwinowski, Z.; Minor, W. *Methods Enzymol.* **1997**, *276*, 307–326.
29. Brünger, A. T.; Adams, P. D.; Clore, G. M.; DeLano, W. L.; Gros, P.; Grosse-Kunstleve, R. W.; Jiang, J.-S.; Kuszewski, J.; Nilges, M.; Pannu, N. S.; Read, R. J.; Rice, L. M.; Simonson, T.; Warren, G. L. *Acta. Crystallogr., D* **1998**, *54*, 905–921.
30. Chrysina, E. D.; Kosmopoulou, M. N.; Tiraidis, C.; Kardakaris, R.; Bischler, N.; Leonidas, D. D.; Hadady, Z.; Somsák, L.; Docsa, T.; Gergely, P.; Oikonomakos, N. G. *Protein Sci.* **2005**, *14*, 873–888.
31. Jones, T. A.; Zou, J. Y.; Cowan, S. W.; Kjeldgaard, M. *Acta Crystallogr., A* **1991**, *47*, 110–119.
32. Laskowski, R. A.; MacArthur, M. W.; Moss, D. S.; Thornton, J. M. *J. Appl. Crystallogr.* **1993**, *26*, 283–291.
33. Collaborative Computational Project No 4. *Acta Crystallogr. D* **1994**, *50*, 760–763.
34. Luzatti, V. *Acta Crystallogr.* **1952**, *5*, 802–810.